Biomedicine & Pharmacotherapy 162 (2023) 114657

Contents lists available at ScienceDirect

Biomedicine & Pharmacotherapy

journal homepage: www.elsevier.com/locate/biopha

New therapy for pancreatic cancer based on extracellular vesicles

Salomé Araujo-Abad [a,b,c], Antonio Manresa-Manresa [a], Enrique Rodríguez-Cañas [b], María Fuentes- Baile [a], Pilar García-Morales [b], Ricardo Mallavia [b], Miguel Saceda [a,b], Camino de Juan Romero [a,b,*,1]

[a] Unidad de Investigación, Fundación para el Fomento de la Investigación Sanitaria y Biomédica de la Comunidad Valenciana (FISABIO), Hospital General Universitario de Elche, Camí de l'Almazara 11, Elche, 03203 Alicante, Spain
[b] Instituto de Investigación, Desarrollo e Innovación en Biotecnología Sanitaria de Elche (IDiBE), Universidad Miguel Hernández, Avda, Universidad s/n, Ed. Torregaitán, Elche, 03202 Alicante, Spain
[c] Centro de Biotecnología, Universidad Nacional de Loja, Avda. Pio Jaramillo Alvarado s/n, Loja, 110111 Loja, Ecuador

ARTICLE INFO

Keywords:
Pancreatic ductal adenocarcinoma
Small EVs
Nanocarriers
Chemotherapy
FESEM

ABSTRACT

Pancreatic Ductal Adenocarcinoma (PDAC), is the most common aggressive cancer of the pancreas. The standard care of PDAC includes tumor resection and chemotherapy, but the lack of early diagnosis and the limited response to the treatment worsens the patient's condition. In order to improve the efficiency of chemotherapy, we look for more efficient systems of drug delivery. We isolated and fully characterized small Extracellular Vesicles (EVs) from the RWP-1 cell line. Our study indicates that the direct incubation method was the most efficient loading protocol and that a minimum total amount of drug triggers an effect on tumor cells. Therefore, we loaded the small EVs with two chemotherapeutic drugs (Temozolomide and EPZ015666) by direct incubation method and the amount of drug loaded was measured by high-performance liquid chromatography (HPLC). Finally, we tested their antiproliferative effect on different cancer cell lines. Moreover, the system is highly dependent on the drug structure and therefore RWP-1 small EVs^{TMZ} were more efficient than RWP-1 small $EVs^{EPZ015666}$. RWP-1 derived small EVs represent a promising drug delivery tool that can be further investigated in preclinical studies and its combination with PRMT5 inhibitor can be potentially developed in clinical trials for the treatment of PDAC.

1. Introduction

Pancreatic ductal adenocarcinoma (PDAC) is a highly aggressive lethal malignancy and the most prevalent type of pancreatic neoplasm. This type of cancer, that develops in the exocrine compartment, accounts for more than 90% of pancreatic cancer cases [1]. It has an average 5-year survival rate of less than 10% and is anticipated to become the third leading cause of cancer–related mortality by 2025 [2], mostly due to the lack of early diagnosis and limited response to treatments [3].

Only a small fraction of PDAC patients can benefit from adjuvant chemotherapy and, especially in advanced stages after tumor resection, chemotherapeutic options are limited, with gemcitabine (Gem) being the first drug treatment or other drugs as 5- fluorouracil with a median survival improvement of only a few weeks [4]. PDAC treatment limitations reinforce the importance of looking for new methodologies, more efficient drugs or drug delivery to be explored and investigated, for the development of novel treatment options.

Temozolomide (TMZ) (3,4-dihydro-3-methyl-4-oxoimidazo-[5,1-d]-astetrazine-8-carboxamide) is a DNA alkylating agent that acts over the methylation of guanine and adenine bases, breaking double-stranded DNA and causing cell cycle arrest and cell death by apoptosis [5]. It has been used to treat glioma, glioblastoma neuroendocrine tumors, melanoma, and sarcomas [6–13] but TMZ treatment has a short half-life

Abbreviations: PDAC,, Pancreatic Ductal Adenocarcinoma; *TMZ,*, temozolomide; *GEM*, gemcitabine; *EVs,*, extracellular vesicles; *BBB,*, blood-brain barrier; *DMEM F-12,*, Dulbecco's Modified Eagle's Medium: Nutrient Mixture F-12; *FBS,*, fetal bovine serum; *MTT,*, methylthiazolyldiphenyl-tetrazolium bromide; FESEM, Field Emission Scanning Electron Microscope; DLS, Dynamic Light Scattering.

* Corresponding author at: Unidad de Investigación, Fundación para el Fomento de la Investigación Sanitaria y Biomédica de la Comunidad Valenciana (FISABIO), Hospital General Universitario de Elche, Camí de l'Almazara 11, Elche, 03203 Alicante, Spain.
E-mail address: m.juan@umh.es (C. de Juan Romero).
[1] ORCID: 0000–0001-7890–8447

https://doi.org/10.1016/j.biopha.2023.114657
Received 24 February 2023; Received in revised form 29 March 2023; Accepted 3 April 2023
Available online 5 April 2023
0753-3322/© 2023 The Author(s). Published by Elsevier Masson SAS. This is an open access article under the CC BY license (http://creativecommons.org/licenses/by/4.0/).

[14] and, to achieve therapeutic levels, high doses are required, with the subsequent appearance of a great number of side effects [15–17].

EPZ015666, is a small-molecule considered a protein arginine methyltransferase-5 (PRMT5) inhibitor. It competes with the substrate binding pocket of PRMT5 peptide to deny its interaction and posterior methylation [18]. PRMT5, which modulates the biological function of target proteins catalyzing the transference of two methyl groups to arginine residues, is essential to maintain homeostasis in both normal and malignant cells [19] and plays an important role in cell development and adult hematopoiesis [20]. PRMT5 is a novel target that has recently emerged for cancer treatment. This enzyme is involved in tumorigenesis and it has been found overexpressed in a variety of cancers including melanoma, multiple myeloma, lung, gastric, prostate, ovarian, colorectal cancers, and glioblastoma [21] and is associated with poor prognosis [19].

Small EVs, that are being secreted from cells into the extracellular space, play an important role in both physiological and pathological processes through interaction with their neighbors and the extracellular environment [22]. Small EVs have a diameter of 30–150 nm [22–24], and a lipid bilayer membrane with the same characteristics of the donor cell [25]. EVs contain mostly RNA, DNA, and proteomic material [25]. Importantly, while the proteins and genetic material may reflect the properties of the parent cells, EVs are generally not mirrored images of the cellular membrane. This suggests that EVs are derived from specific subcellular locations, and their contents are likely intended for a defined function in the extracellular space.

One of the most important characteristics to be explored of small EVs is their use as drug delivery carriers. Small EVs have some advantages over synthetic systems (liposomes, dendrimers, nanoparticles, etc.), like, specific tropism for cell origin [26], non-cytotoxic effect, biocompatibility, facility of transporting either hydrophilic or hydrophobic biomolecules and facility to cross the blood-brain barrier (BBB) [27,28]. These novel nanocarriers can contribute to increasing the efficiency of PDAC treatment.

The advanced age of most PDAC patients explains the lack of satisfactory results, as postoperative systemic therapy may not be ideal for these individuals. The patient's systemic contact with chemotherapeutics at high concentrations exposes them to an increased risk of systemic toxicities, affecting their overall well-being [29]. Localized interventions, however, retain cytotoxic agents at a specific site, thus reducing drug exposure and decreasing toxicity while maximizing treatment efficacy. In recent years, there has been considerable interest in the use of localized drug delivery systems to perform localized interventions as alternatives to systemic therapy [30].

In the present study, we focused on small EVs released from RWP-1 cells. We described an efficient and reproducible method of small EVs purification, performing as well several characterization methods in order to ensure its purity. We have used those small EVs to overcome the present challenges of treatment and drug delivery in PDAC. We have used TMZ and EPZ015666 to demonstrate that small EVs derived from RWP-1 have target specificity, and that those drugs loaded into small EVs inhibit the proliferation of PDAC cells in vitro at less concentration exposure than when they are directly applied. Therefore, RWP-1-derived small EVs could be used as a nanocarrier for the development of new therapeutic strategies.

2. Materials and methods

2.1. Cell culture

Pancreatic adenocarcinoma cell line (RWP-1), was donated by Instituto Municipal de Investigaciones Médicas (IMIM, Barcelona, Spain) [31]. Isolation of primary human GBM cell line (HGUE-GB-39) was performed from surgical washes as previously reported [32,33]. The GBM cell line, HGUE-GB-39 and RWP-1 were cultured as previously described [31–33].

2.2. Proliferation assays

Methylthiazolyldiphenyl-tetrazolium bromide (MTT) assays were performed to analyze the antiproliferative effect of the drugs and the EVs. Cells were seeded in 96-well standard plates (Sarstedt, Nümbrecht, Germany) with a density of 4000 cells/well and incubated at 37 ºC and 5% CO_2 for 24 h. Then, cells were either treated with different and increasing concentrations of the TMZ, EPZ or loaded small EVs and incubated for 72 h under the same conditions. After that, 0.25 mg mL^{-1} of MTT (Sigma-Aldrich, MO, USA) was added and incubated for 3 h, media was carefully removed and 100 μL of dimethyl sulfoxide (DMSO) (Sigma-Aldrich, MO, USA) was added. To dissolve the formazan crystals, the plates were vigorously shaken at room temperature for 20 min. Finally, the absorbance was measured on an Eon™ Microplate Spectrophotometer (BioTeK®, Winooski, VT, USA) at 570 nm.

2.3. Small EVs purification

Confluent populations of RWP-1 and HGUE-GB-39 cell lines were incubated in T75 flasks with DMEM-HG and DMEM F-12 conditioned media respectively. After 4 days small EVs were obtained by differential ultracentrifugation method. The media samples were centrifuged at 2000 x *g* for 20 min at 4 ºC to eliminate cells and debris followed by an initial ultracentrifugation using Optima L-90 K Ultracentrifuge (Beckman Coulter) with 70.1 Ti rotor at 25,000 x *g* for 40 min at 4 ºC to remove macrovesicles then the supernatant was filtered through 0.22 μm filters (Fisher Scientific). The resultant filtrate was centrifuged at 110,000 x *g* for 90 min at 4 ºC to pellet small EVs that were then washed in PBS at 110,000 x *g* for 90 min at 4 ºC and the final pellet was resuspended in 200 μL of 1X PBS and then stored at − 80 ºC.

2.4. Western blot

An amount of 10 μg of total protein was solubilized with loading buffer (4x) (2-mercaptoethanol + NuPage; 1:5) and heated at 95 ºC for 5 min for reducing conditions and without 2-mercaptoethanol for non-reducing conditions. Then, proteins were separated by SDS-PAGE using 10% gels and transferred to a Nitrocellulose membrane (Bio-Rad Laboratories Inc, California, USA). Membranes were incubated overnight at 4 ºC with primary antibodies: anti-CD63 (mouse,1:1000, Invitrogen), anti-ALIX (mouse,1:500, Invitrogen), anti-TSG101 (mouse,1:500, Invitrogen), anti-α-tubulin (mouse, 1:10000, Invitrogen) and anti-HSP90-B1 (rabbit,1:4000, CUSABIO) followed by one hour incubation at room temperature with ECL™ Anti-mouse IgG and ECL™ Anti-rabbit IgG, Horseradish Peroxidase linker (GE Healthcare, UK). The membranes were visualized with ECL™ Prime Western blotting detection reagent (Amersham™) in the ChemiDoc Bio-Rad instrument [33].

2.5. Dynamic light scattering (DLS)

To characterize size distribution, RWP-1 small EVs samples were analyzed using a Zetasizer Nano ZS instrument (Malvern Panalytical). Each sample was diluted in Milli-Q™ water (1:10), 1 mL was dispensed in a polystyrene disposable cuvette (Zen0040) and read at least seven times in Zeta sizer Software. The final image with the distribution curves was used in the figures as an illustrative example of the medium size (Fig. 1B).

2.6. Field emission scanning electron microscope (FESEM)

RWP-1 small EVs were fixed with Paraformaldehyde 2%, sonicated for 5 min and diluted in serial dilutions with Milli-Q™ water (1:10; 1:100; 1:1000, 1:10000). A 50 μL sample droplet was deposited on a silicon wafer and, once evaporated, the samples were observed using a Zeiss Sigma 300 VP Field Emission Scanning Electron Microscope (FESEM) without coating (Fig. 1C). EVs morphology was analyzed at

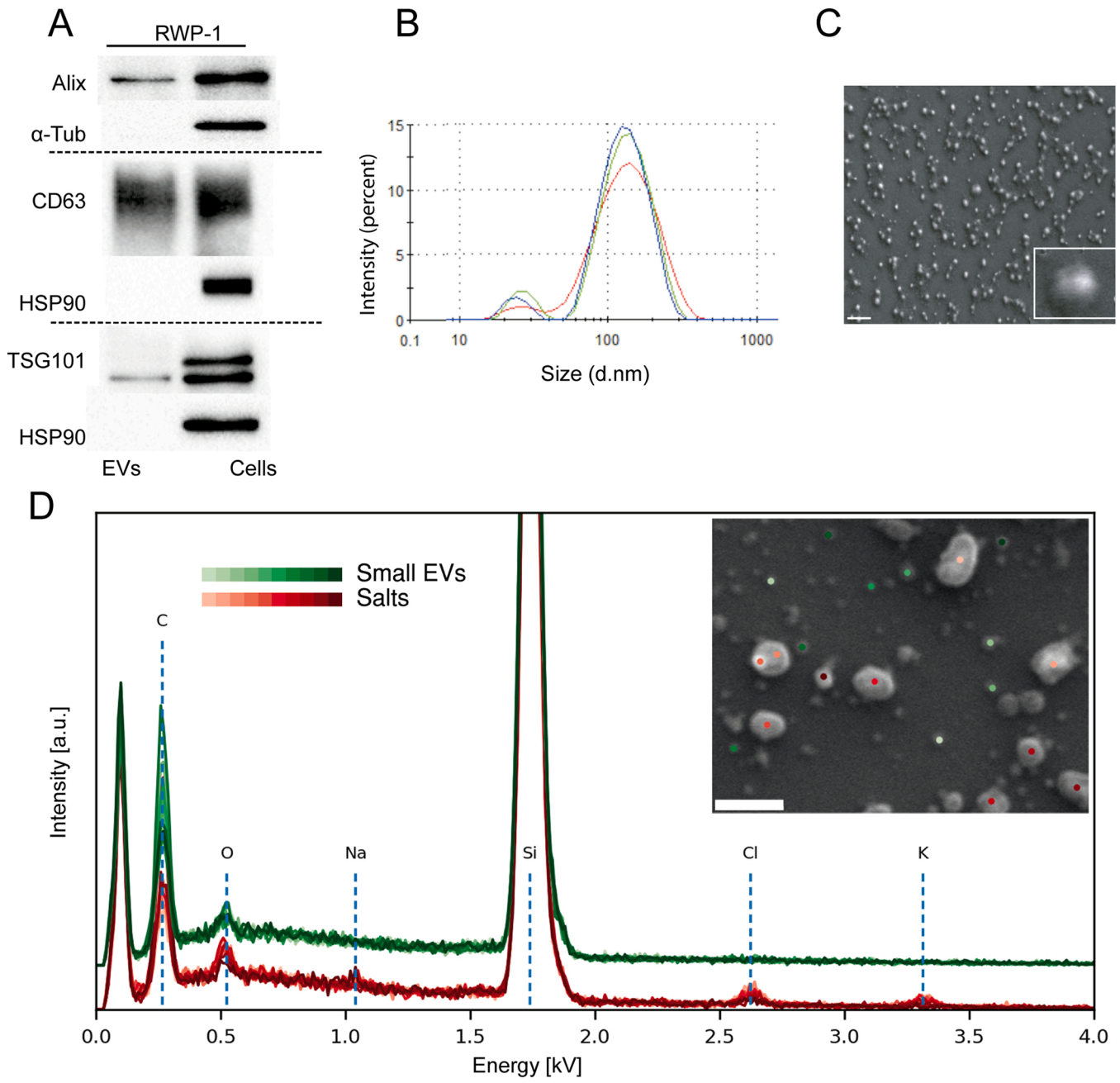

Fig. 1. Biochemical and biophysical characterization. **A** Expression by WB of Alix, CD63, and TSG101 in small EVs and RWP-1 cell line. α-Tub and HSP-90 were used as control. **B** Size and morphology of the RWP-1 cell line derived small EVs were visualized using Dynamic light scattering (DLS) and (**c)** Field Emission Scanning Electron Microscopy (FESEM). **C** Energy dispersive X-ray (EDX) analysis was performed with the X-ray detector in a FESEM microscope on one of the EVs samples. The studied samples were a mixture of biological samples and salts. Green color indicates the location of the EVs analysis and red color salts. The spectrum of each of the areas was done at 3.5 kV in order to maximize the contribution of the EVs and minimize the contribution of the silica peak (Si) which corresponds to the substrate and is present in both samples. Blue chopped lines point at different inorganic elements present in salt crystals but not in the EVs. Scale bar 0.5 μm. EVs, extracellular vesicles; FESEM, Field Emission Scanning Electron Microscope White boxes show an optical magnification of a representative small EV. Scale bars 200 nm.). EVs, extracellular vesicles.

low voltages around 1 kV while higher voltages were employed to differentiate the salts from the biological sample using Energy Dispersive X-ray (EDX) (Fig. 1D).

2.7. Small EVs labelling

The CellVue® Claret Far Red Fluorescent kit (Sigma-Aldrich, MO, USA) was used to label small EVs. 200 μL of RWP-1 small EVs, were treated with the kit content following manufacturer's instructions. After being washed twice in PBS with 110,000 x *g* centrifugation, the labeled small EVs were filtered with 0.2 μm and resuspended in PBS prior to be used.

2.8. Immunocytochemistry (ICC)

An amount of 35,000 cells of RWP-1 cell line were seeded into twenty-four-well plates on coverslips. After, cells were treated for 6 h with red labeled RWP-1 small EVs, fixed with paraformaldehyde at 4% concentration, and blocked with FBS/PBS (1X) (50 μL/mL). Then, cells were incubated with anti-E-cadherin (1:100, rabbit, Invitrogen,

Barcelona, Spain) primary antibody. After washing out the first antibody, cells were incubated with Alexa Fluor 488-labeled anti-rabbit (1:500) secondary antibody (Invitrogen, Barcelona, Spain); the DAPI (4′,6-diamidino-2-phenylindole) reagent from Sigma (Madrid, Spain) was used to stain the nucleus. Coverslips were mounted in Prolong™ Gold Antifade Reagent (Invitrogen, Barcelona, Spain) and analyzed using a Zeiss Axioscope 5 microscope with the LED light source Colibri 3 (Carl Zeiss, Oberkochen, Germany).

2.9. Small EVs drug-loading

RWP-1 small EVs were loaded with two different procedures, direct and indirect incubation. For the first method, small EVs were incubated for 2 h at 37 ºC in a thermoblock with defined concentrations of a given chemotherapeutic drug (EPZ015666 15 μM or TMZ 5 mM). Then, they were washed with PBS 1X and ultracentrifuged at 110,000 x *g* for 60 min at 4 ºC to pellet the loaded small EVs. Finally, they were filtered with a 0.22 μm membrane under sterile conditions and stored at − 80 ºC. The indirect procedure consisted in the incubation of GBM cell culture with the drug of interest (EPZ015666 15 μM or TMZ 5 mM) for 72 h. Then, the flasks were treated as previously described in the small EVs purification section.

2.10. Quantification of TMZ and EPZ015666 by HPLC

The amount of TMZ and EPZ015666 loaded into the small EVs was determined by the high-performance liquid chromatography (HPLC) method. Briefly, 200 μL of small EVs were placed in a Concentrator plus (Eppendorf, Germany) at 40ºC for 2 h to evaporate the solvent. Then, 100 μL volume of acetonitrile was added, and the mixture was vortexed, sonicated and then centrifuged at 13,200 x *g* (Centrifuge 5415 R, Eppendorf) for 10 min. After centrifugation, the supernatant was transferred into HPLC vials and injected into the UPLC-QtoF-MS/MS equipment with a high-resolution flight tube and quadrupole technology (Waters- Bruker). Detection of TMZ and EPZ015666 were optimized with a Waters I-Class with UV detection at 330 and 254 nm respectively, followed by the use of QToF-MS de Bruker Daltonics, maXis impact Series model in positive ionization mode by Electrospray (ESI) with column ACE Excel C18-Ar (50–3; 1.7 μm). The mobile phase used was: A) Water with 0.1%v/v acetic acid and B) Methanol with 0.1% acetic acid. Gradient: 0 min, 95% A; 5.50 min, 60% A, 8.75 min, 5% A, with a flow rate of 0.3 mL/min and an injection volume of 5 μL.

2.11. Live cell imaging

For live imaging of small EVs uptake, RWP-1 cells were seeded in 96-well black plates with clear bottoms (Corning, Kennebunk, ME, USA) with a density of 16000 cells/well and incubated at 37ºC and 5% CO_2 for 24 h. Then, cells were treated with red labeled RWP-1 small EVs^{TMZ} and incubated for 3 and 6 h under the same conditions. After that, cells were rinsed with (1X) PBS twice and then placed in a Cytation 3 (BioTeK®, Winooski, VT, USA) instrument to take the images. Images were exported as a tiff file format for further analysis in Fiji software.

2.12. Statistical analysis

Results were expressed as mean ± standard deviation (SD) of three independent experiments. In order to evaluate the normal distribution of the data, Shapiro-Wilk statistical test was used, and the statistical significance was determined by Student's t-test or the Mann-Whitney U test. Differences were considered to be statistically significant with a *p*-value of less than 0.05. Statistical analysis was performed with GraphPad Prism v7.0a software (GraphPad Software Inc., San Diego CA, USA).

3. Results

3.1. Small EVs isolation and biochemical characterization from a pancreatic cancer cell line

In order to study the role of tumor derived small EVs, we have used one of the two human pancreatic cancer lines, RWP-1 and RWP-2, that were established from patients with primary pancreatic cancer metastatic to the liver [34]. In this work, we are using RWP-1, which has moderately well differentiated ductal cell adenocarcinoma features, and has been used as a model cell line for pancreatic ductal adenocarcinoma in several studies [34–38]. If an effect is observed in this PDAC cell line, we will check if it is specific to this cancer type. Therefore, we also used the radioresistant GBM, GB-39 cell line, obtained from a patient's primary culture [32].

We isolated a small EVs sample from RWP-1 by ultracentrifugation protocol for further biochemical and biophysical characterization. RWP-1 and GB-39 small EVs were used in functional studies. Characterization of small EVs derived from RWP-1 has been standardized for reliable and reproducible results from assays and other downstream applications. We have used Western Blot (WB) as an analytical technique to detect specific proteins in a sample of small EVs, as well as a semi-quantitative estimation of the protein content. We have identified the presence and expression level of Alix, CD63, and TSG101, the most commonly used proteins in small EVs characterization. Our results showed their presence in small EVs derived from RWP1, while α-Tubulin and HSP-90 were only found in cell lysates (Fig. 1A). Given that the proteins and genetic material inside the small EVs may reflect properties of the parent cells [39], our results established a high purity of the RWP-1-derived small EVs samples that will be used in functional experiments.

3.2. Morphological and physical characterization of RWP-1-derived small EVs

DLS was used on RWP-1-derived small EVs (Fig. 1B) to analyze the size of the isolated vesicle population. Our results showed that the isolated particles had a medium size of: 141.5 ± 4.4, consistently within the expected size range for small EVs (Fig. 1B). We further examined the size and morphology of RWP-1-derived small EVs by performing FESEM analyses (Fig. 1C). FESEM images indicated the presence of a homogeneous population of small EVs with diameters of 100–150 nm, with a round or cup shaped morphology. To rule out that the structures visualized by FESEM could be an artifact of the isolation or fixation process, we performed an energy dispersive X-ray (EDX) analysis. The X-ray detector in a FESEM microscope was used on RWP-1-derived small EVs sample (Fig. 1D) for 10 times. The X-ray detector was placed on several structures of the sample, confirming that the studied sample was a mixture of organic samples and salts. All the samples showed a silica peak corresponding with the substrate. The spectrum of the rounded small EVs like areas, showed a high content in carbon and oxygen confirming their organic origin. Areas corresponding to salts presented a chloride and potassium content. In line with similar studies uncovering small EVs characteristics, DLS and FESEM imaging confirmed the presence and purity of RWP-1-derived small EVs in our preparations [40]. Moreover, the EDX analysis established the organic nature of RWP-1 derived small EVs samples (Fig. 1D). Finally, since the small EVs will be loaded with different drugs, it was interesting to see that they keep their round shape after isolation (Fig. 1B) and that they have a considerable and well established size (Fig. 1C) that can be reproducible.

3.3. RWP-1 drug resistance profile

PDAC is one of the most lethal diseases, mostly because the majority of patients have unresectable, locally advanced, or metastatic disease at the time of diagnosis. Unfortunately, traditional treatments such as surgery, chemotherapy and radiation lead to modest improvements in

postoperative survival due to the high prevalence of drug-resistant phenotypes [41]. Moreover, since chemotherapy is all too often associated with toxicity, many patients elect for palliative care [42]. At the moment the standard of care is the use of Gem alone or in combination with other drugs such as 5-Fluorouracil, Leucovorin, Irinotecan, and Oxaliplatin, although it shows marginal efficacy in clinical trials [43–45]. Since there is currently no effective treatment for PDAC, it is essential to find new alternative drugs and new delivery systems that enhance drug efficacy and extend patient survival while improving quality of life.

The alkylating agent TMZ is a treatment option for several solid tumors such as glioma, glioblastoma, neuroendocrine tumors, melanoma, and sarcomas [6–13]. However, when TMZ has been used in an advanced untreated pancreatic cancer phase II study, it is not a standard of care due to its high cytotoxicity and low effect on patients [13]. We hypothesize that if it could reduce the side effects of systemic exposure to TMZ, this drug could also be a therapeutic option for PDAC patients. The effect of TMZ treatment on proliferation was assessed using an increasing concentration of the drug. We evaluated a range of concentrations between 0.05 mM and 10 mM. Our analyses revealed that treatment of the RWP-1 with TMZ resulted in more than 75% decreased proliferation, together with an IC_{50} of 0.7301 ± 0.066 (Fig. 2A).

As mentioned before, Gem has been used since 1983, constituting the first-line chemotherapy for most PDAC patients and forming the backbone of several drug combinations [46]. Recent studies have revealed that protein arginine methyltransferase gene 5 (PRMT5) is a promising druggable candidate whose inhibition creates synergistic vulnerability of PDAC cells to Gem [47]. EPZ01666 is the inhibitor of PRMT5, which has been shown to regulate the splicing of detained introns in proliferation-associated genes in GBM[48] and has been broadly used in several types of cancer [18,49]. In this study, we are testing the effect of both treatments, TMZ but also new therapies like EPZ015666, on the RWP-1 cell line.

The effect of the EPZ015666 treatment on proliferation was assessed using an increasing concentration of the drug. We evaluated a range of concentrations between 10 μM to 60 μM. Our analyses revealed that treatment of the RWP-1 with EPZ015666 resulted in more than 60% decreased proliferation, together with an IC_{50} of 23.31 ± 0.064 (Fig. 2B).

3.4. Loaded GBM derived small EVs decrease RWP-1 cell proliferation

In order to test which incubation method is better for drug loading, GB-39 derived small EVs were loaded by two incubation methods [50]. For indirect incubation, the GB-39 cell line was treated for 72 h with high doses of TMZ or EPZ015666 and small EVs were isolated from the medium (Fig. 3B). For direct incubation protocol, small EVs were first isolated from GB-39 and then incubated in a medium containing a low dose of either of the proposed drugs (Fig. 3A).

Small EVs were loaded by direct and indirect incubation with 5 mM of TMZ, and the loading efficiency of GBM derived small EVs was determined by measuring the amount of TMZ within the EVs by HPLC. Our HPLC measurements showed a higher amount of TMZ being loaded into the small GBM derived EVs by direct incubation (data not shown).

Next, we wonder if small EVs can be used as a drug delivery system for PDAC cancer treatment. When applying the TMZ loaded small EVs on the RWP-1 cell line, direct incubation showed no significant differences as compared with indirect incubation, although both incubation methods have a mild effect on tumor pancreatic cells (Fig. 3C). However, EPZ015666 has a significant effect in RWP-1 cells, direct incubation being the most effective loading method (Fig. 3D). This reduction in proliferation is very important since the small EVs were loaded with only 0.04 μM and they were applied in concentrations that range from 0.002 to 0.02 μM.

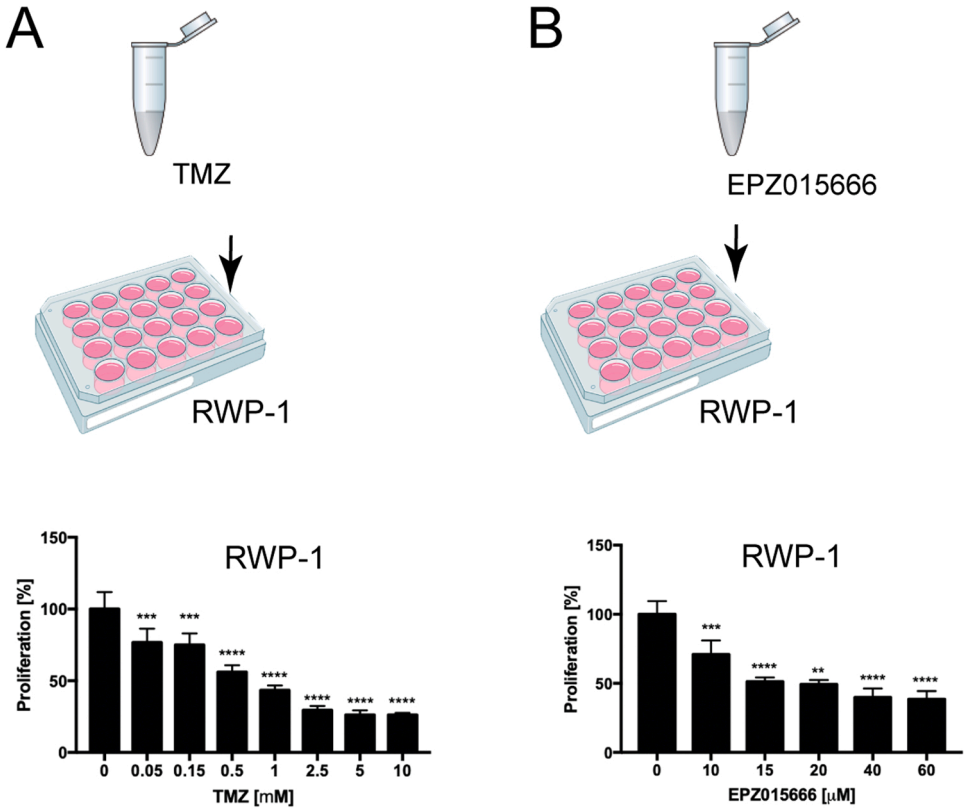

Fig. 2. Cell proliferation effect of TMZ and EPZ015666 in RWP-1 cell line. **(A)** Cancer cells were treated with increasing concentrations of TMZ and **(B)** EPZ015666 and their effect over cell proliferation was measured. Asterisks indicate the statistical significance of the results (** $p < 0.01$, *** $p < 0.001$, **** $p < 0.0001$). TMZ, Temozolomide.

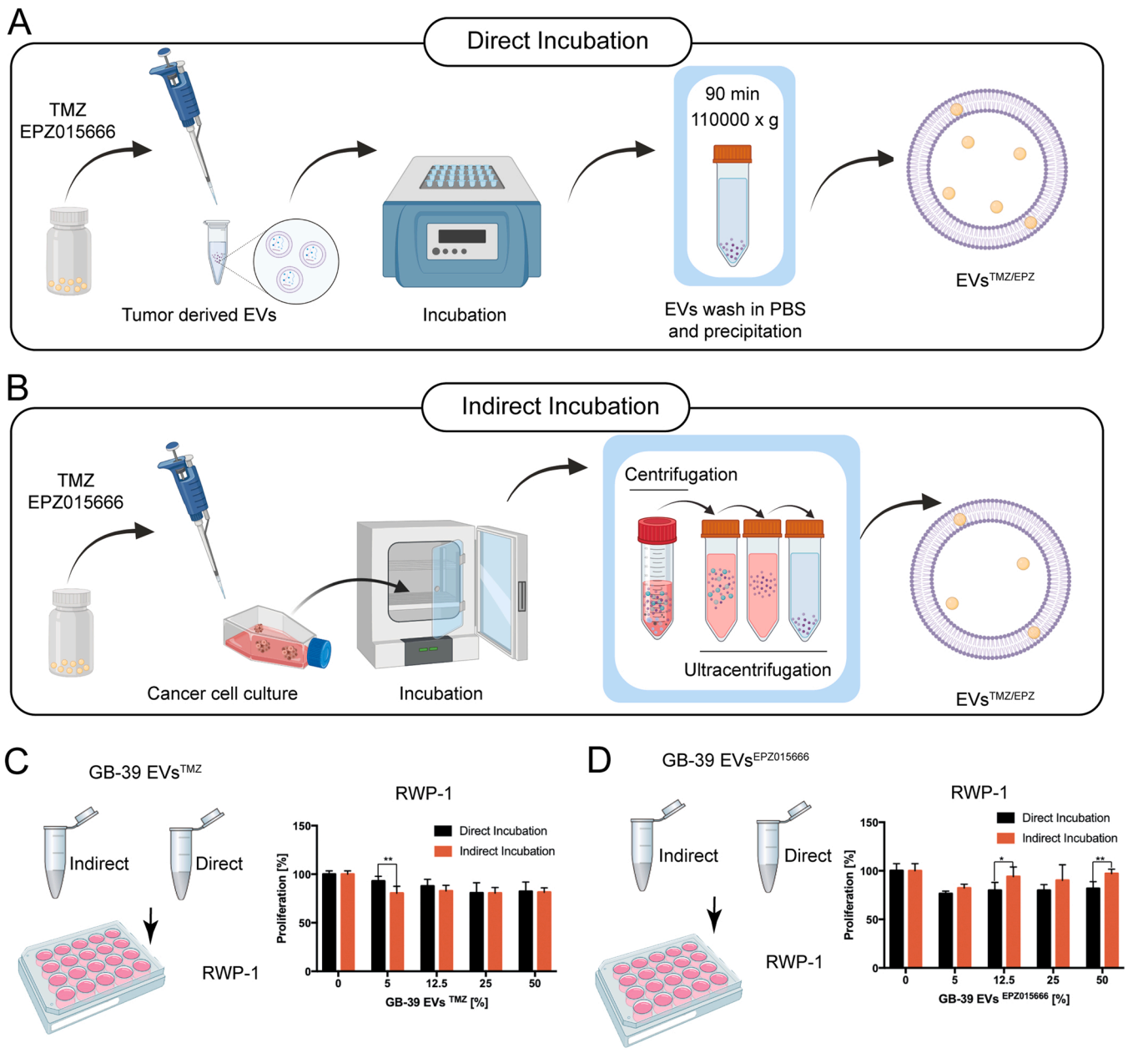

Fig. 3. Drug loading of small EVs particles. A Scheme representing the sequential steps for small EVs loading using the direct method. **B** Scheme representing the sequential steps for small EVs loading using the indirect method. **C** Comparison of the effect on cell proliferation of GB-39^{TMZ} small EVs using direct (black bars) and indirect (red bars) loading methods. **D** Comparison of the effect on cell proliferation of GB-39^{EPZ015666} small EVs using direct (black bars) and indirect (red bars) loading methods. Asterisks indicate the statistical significance of the results (* $p < 0.05$, ** $p < 0.01$).

Taken together, direct incubation was a better method to load the small EVS (Fig. 1C-D) and, for the first time, the effect of PRMT5 drug inhibitor has been tested on a cancer cell line derived from a patient with pancreatic adenocarcinoma. Our results show not only the potential therapeutic effect of EPZ05666, but also the increase in the efficacy of both drugs as indicated by the decrease in cell proliferation at very low doses (Fig. 3C-D).

3.5. TMZ shows more efficiency when loaded in RWP-1-derived small EVs

It has been proposed that small EVs have directionality toward their mother cell [26]. Therefore, we speculate that small EVs derived from RWP-1 may have a higher effect on their cells of origin, than the GBM derived small EVS. To test this idea, we used the isolated small EVs from the RWP-1 cell line to load them with the proposed drugs. We used the direct incubation method in our experiment to load the vesicles, using a concentration of 5 mM for TMZ (RWP-1 EVs^{TMZ}) and 15 μM for EPZ015666 (RWP-1 EVs^{EPZ015666}) for the incubation.

In order to know the precise amount of drug contained in the small EVs, we performed an HPLC analysis followed by drug identification with a mass spectrometer (Fig. 4A). Our quantifications showed that RWP-1 EVs^{TMZ} were loaded with 7.2 μM. Isolated RWP-1 EVs^{TMZ} were applied to the cells in serial dilutions ranging from 50% to 5% of the original stock. Since the amount of drug applied to the cultures throughout the RWP-1 EVs^{TMZ} corresponds to a range that goes from 3.6 μM to 0.36 μM, we tested the direct exposure of the RWP-1 cell line to TMZ at these low concentrations to compare both effects (Fig. 4C). The maximum concentration applied was 3.6 μM of TMZ corresponding to 50% of RWP-1 EVs^{TMZ} and the minimum was 0.36 μM at 5% of TMZ.

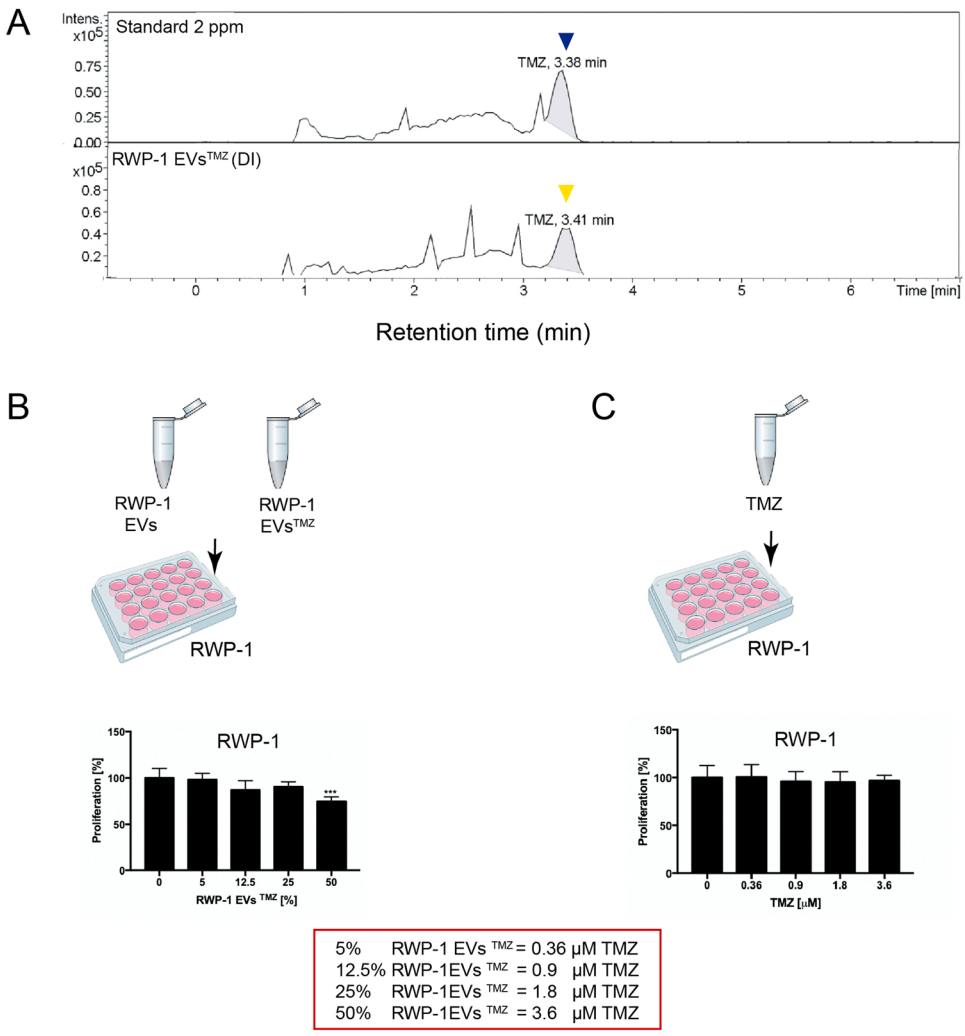

Fig. 4. HPLC-MS analysis of small EVs sample RWP-1 EVs^{TMZ} and cell proliferation effect. A The amount of TMZ incorporated into small EVs was quantified by HPLC. The dark blue arrow indicates the standard TMZ (2 ppm) at 3.38 min retention time. The yellow arrow indicates the RWP-1 EVs^{TMZ} sample (Direct Incubation) (1.405 μg/mL) at a retention time of 3.41 min **B** Small EVs of RWP-1 were loaded directly with a 5 mM concentration of TMZ (RWP-1 EVs^{TMZ}). Small EVs alone or serial dilutions of RWP-1 EVs^{TMZ} were applied to RWP-1 cell line and their effect on proliferation was measured. **C** Cancer cells were treated with increasing concentrations of TMZ and their proliferation was measured. The red box indicates the equivalence of concentrations. Asterisks indicate the statistical significance of the results (*** $p < 0.001$). TMZ, Temozolomide; EVs, extracellular vesicles.

RWP-1 EVs^{TMZ} treatment resulted in a dose dependent reduction in cancer cell proliferation. Interestingly, the application of the drug using RWP-1 EVs^{TMZ} resulted in a more significant effect on RWP-1 cell proliferation with 25.6% than the reduction produced by GB-39 EVs^{TMZ} by only 17.7% (Fig. 3C, Fig. 4B), supporting the idea that small EVs have tumor tropism to their mother cell.

It has been shown that the best way to maintain the structure and functionality of the EVs is to keep them at − 80 ºC [51]. Therefore, we also analyzed the stability of the drug loaded EVs over long term storage. We repeated the same experiments after two years of keeping EVs^{TMZ} under − 80 ºC conditions and we observed only a decrease of 4% efficiency in the case of TMZ and 10% decrease in EPZ015666 (Fig. S4), These results corroborate that the storage at − 80 ºC is appropriate but the stability also depends on the drug.

Our results indicate that the total amount of TMZ used for the treatment with EVs was up to a hundred and fifty times lower than the direct application of TMZ in cells (Fig. 2A, Fig. 4B). This is very important because when TMZ was applied to the cells directly, at the very same RWP-1 EVs^{TMZ} treatment concentrations, it had no significant effect in cell proliferation (Fig. 4C). All these data indicate that RWP-1 EVs^{TMZ} treatment not only increases the target directionality but also the efficiency of the drug.

3.6. Small EVs incorporation by their mother cell

It has been shown that small EVs have tropism for their mother cell [26,38]. In order to see how the loaded small EVs were incorporated into RWP-1, we treated this cell line with red labeled RWP-1 small EVs^{TMZ} in unfixed cells, for 3 and 6 h. As shown in the figure (Fig. 5A) small EVs ^{TMZ} tend to aggregate in the cytoplasm but mostly in the nucleus after 6 h of treatment. Besides, after 6 h of incubation, the number of small EVs/ cell significatively increases (Fig. 5B). At 6 h of treatment, immunocytochemistry showed that the internalized small EVs were in the cytoplasm, aggregated around the nucleus, as shown by DAPI and E-Cad staining (Fig. S2).

3.7. EPZ015666-loaded RWP-1-derived small EVs have a similar effect on cancer cells

Given that PDAC patients' median survival rate is only 6 months, and more than 93% of patients die within the first 5 years [52], many efforts have been made to find novel drug combinations that will synergistically increase Gem's therapeutic effects. Using a multiplex CRISPR gene KO screening technology with a library of sgRNAs to screen chromatin regulators whose depletion may create conditional lethality with Gem, Wei and colleagues have recently shown that PRMT5 is a significant therapeutic target in PDAC patients who mostly receive Gem as a chemotherapeutic agent [47].

To test the effect of the EPZ015666 treatment on proliferation, increasing concentrations of the drug were used. Small EVs were loaded by direct incubation in 15 μM EPZ015666 (RWP-1 EVs^{EPZ015666}). Similar to the previous experiments, the HPLC analysis followed by drug

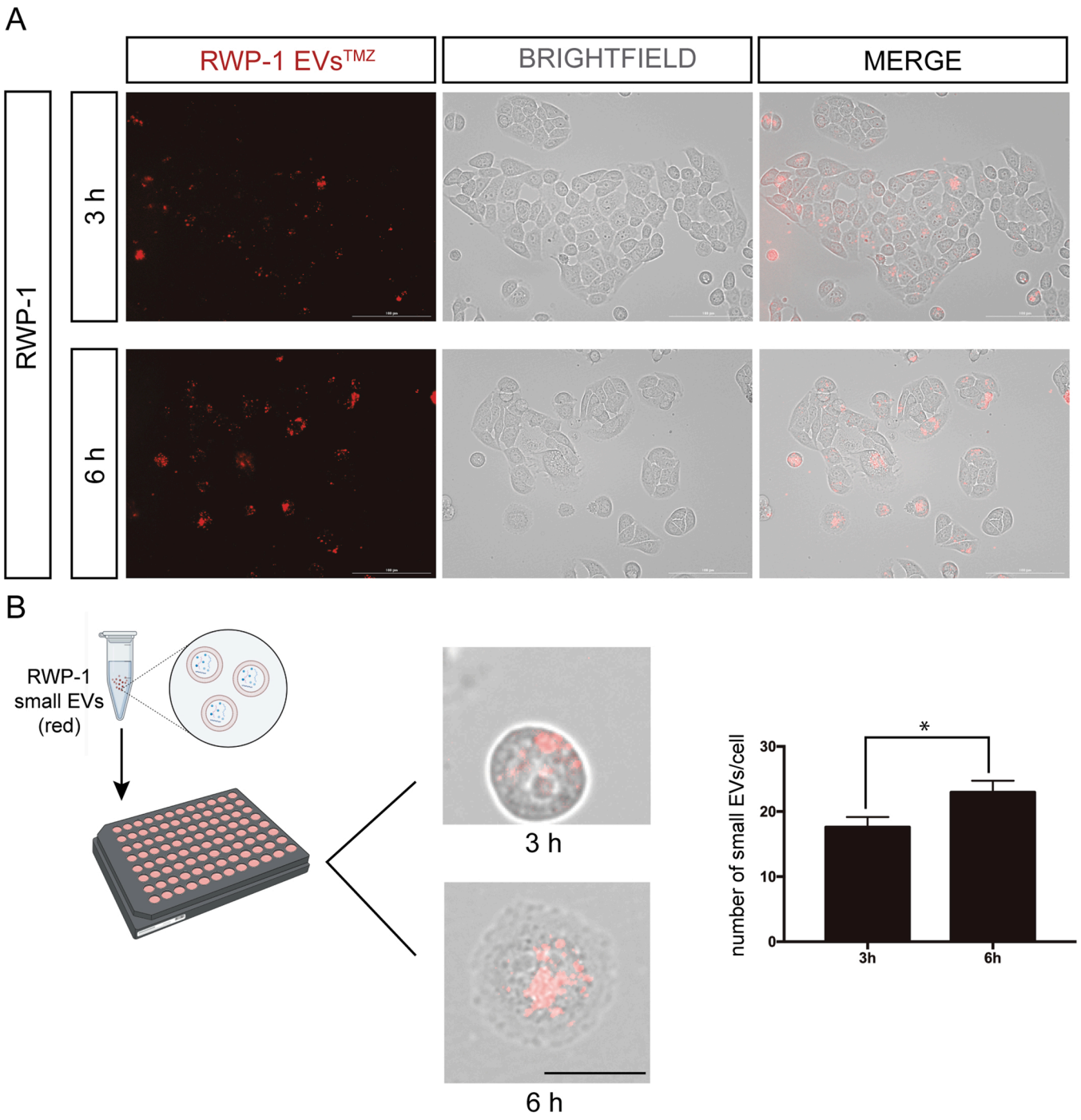

Fig. 5. RWP-1 small EVs internalization in living cells. A RWP-1 cells (Brightfield) were incubated with RWP-1 small EVs^{TMZ} (red) at 3 and 6 h. A representative experiment is shown ($n = 6$). **B** Scheme representing the treatment with RWP-1 small EVs (red). The Fiji software was used to account for the number of small EVs (red dots). Data represent mean ± SEM, Student's 2-tailed unpaired t-test was used, *p < 0.05. Scale bars: A,1000 μm; B, 20 μm.

identification with a mass spectrometer was performed (Fig. 6A). Our quantifications showed a 0.05 μM concentration in the small RWP-1 EVs^{EPZ015666} by direct incubation. Therefore, those samples were loaded with a concentration that was three hundred times lower than the original 15 μM. We wonder if EPZ015666 could have different target efficacy based on the cell origin of the small EVs. Therefore, isolated small RWP-1 EVs^{EPZ015666} were applied to the RWP1 and GB-39 cells in serial dilutions ranging from 50% to 5% of the original stock (Fig. 5B, Fig. S1). Consequently, the maximum concentration was 0.02 μM corresponding to 50% small EVs and the minimum was 0.002 μM when 5% of EVs^{EPZ015666} were applied (Fig. 6B). Direct administration of the drug showed a nearly 60% decrease in proliferation in RWP-1 at high doses (60 μM) (Fig. 2B) however, at the low concentration corresponding to the amount loaded inside the small EVs, EPZ015666 didn't have any effect (Fig. 5C).

RWP-1 EVs^{EPZ015666} application resulted in an average of 16% reduction in proliferation on the RWP-1 cell line. Contrary to the RWP-1 EVs^{TMZ} effect, this reduction was observed regardless of the small EVs concentration (Fig. 6B). It has been shown that different drugs with different mechanisms of action and chemical properties could be more suitable for small EVs drug delivery. We could observe that TMZ-loaded in RWP-1 EVs was more efficient than EPZ015666, indicating that TMZ

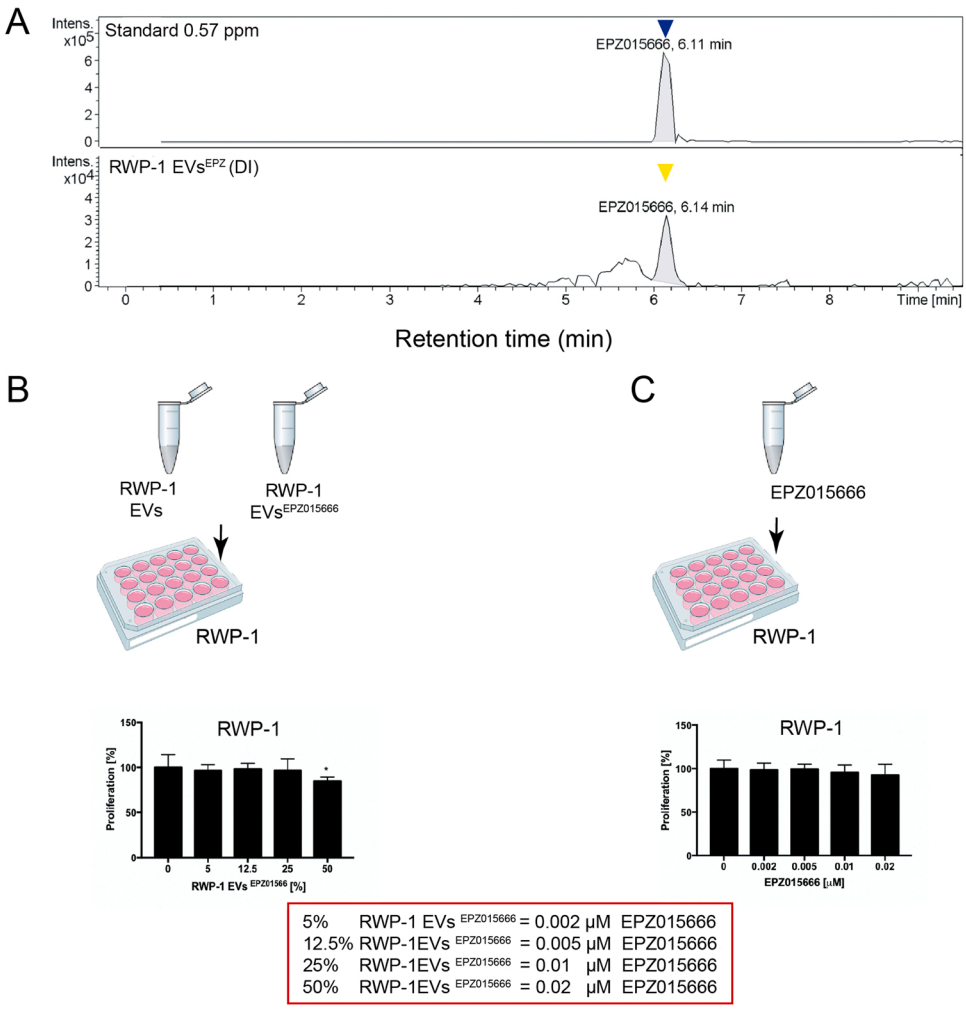

Fig. 6. HPLC-MS analysis of small EVs sample RWP-1 EVs^{EPZ015666} and cell proliferation effect. A The amount of EPZ015666 incorporated into small EVs was quantified by HPLC. The dark blue arrow indicates the standard EPZ015666 (0.57 ppm) at a 6.11 min retention time. Yellow arrow indicates the RWP-1 EVs^{EPZ015666} sample (Direct Incubation) (0.02 µg/mL) at 6.14 min retention time. **B** Small EVs of RWP-1 were loaded directly with a 15 µM concentration of EPZ015666 (RWP-1 EVs^{EPZ015666}). Small EVs alone or serial dilutions of RWP-1 EVs^{EPZ015666} were applied to RWP-1 cell line and their effect on proliferation was measured. **C** Cancer cells were treated with increasing concentrations of EPZ015666 and their proliferation was measured. The red box indicates the equivalence of concentrations. Asterisks indicate the statistical significance of the results (*** $p < 0.001$). EVs, extracellular vesicles.

has better interaction with the lipid bilayer of the small EVs membrane as previously reported for other compounds [53]. Therefore, our results indicate that even if the amount of EPZ015666 that reaches the cell is sufficient to induce an effect, RWP-1 derived small EVs are not suitable to be loaded with EPZ015666 for PDAC therapy.

4. Discussion

Endocrine pancreatic cancers are generally more indolent tumors with a more favorable prognosis as compared with exocrine cell tumors, most commonly pancreatic ductal adenocarcinomas. Since PDAC constitutes approximately 95% of pancreatic cancers, the fundamental challenges that underlie the high mortality of this type of cancer are: 1) Pancreas location. As the pancreas is situated deep within the upper abdomen and only 15–20% can undergo surgical resection. As the pancreas is located between the aorta and its major upper abdominal branches, it is difficult to visualize growing tumors and cancer often grows around the vessels, wrapping them. 2) Early metastasis. More than 50% of PDAC patients develop distant metastasis and the majority of patients who undergo resection will develop metastases within 4 years of surgery [54–57]. 3) Wasting syndrome. At diagnosis, 80% of patients with PDAC, have a reduced ability to withstand aggressive treatment due to the physiologic effects of PDAC [58]. The poor treatment tolerance is evidenced by decreased survival of those patients after pancreatectomy or chemotherapy [59–63]. In order to improve the treatment of these patients it is necessary to find not only new treatments but also new delivery approaches to reduce the side effects.

In this study, we used several sources of small EVs and presented evidence that direct incubation was a better method to load the small EVS (Fig. 1C-D). Thus, when RWP-1 pancreatic tumor cell line is exposed to GB-39 EVs loaded with TMZ or EPZ015666, it undergoes a lower decrease in proliferation than when loaded RWP-1 EVs are applied. This data supports the idea that small EVs derived from RWP-1 are a more efficient drug carrier than GB-39 EVs.

In this study, we demonstrated that EVs derived from RWP-1 are good drug carriers for PDAC treatment, providing more efficiency than direct administration at very low doses. Moreover, in this work we have shown that small EVs have target specificity, having a higher impact on proliferation when they are isolated from the same type of tumor cell.

The uptake of the RWP-1 EVs^{EPZ015666} by the pancreatic tumor cells was not dose-dependent, indicating that RWP-1 small EVs were not a good carrier for this drug. The fact that the direct application of EPZ015666 has a great impact on RWP-1 suggests that it could be a good therapy for PDAC, although it should be mobilized by other means such as nanoparticles (Fig. 2B).

Several groups have extensively studied how the storage conditions affect the morphology and functionality of the EVs [51,64–66]. We have observed that both tested drugs not only behave differently and have different loading capacities, but also present different long-term stability.

The fact that the benefit associated with the use of this natural nanocarrier depends on the type of the used drug, probably relies on the different interactions between the chemical structure of the drug and the extravesicular membrane, and this interaction will define its

internalization. Along this line, our data indicate that RWP-1 EVs^{TMZ} was more efficient than RWP-1 $EVs^{EPZ015666}$, suggesting that TMZ has better interaction with the lipid bilayer. This opens a new field of study, to investigate which drugs can be better loaded into small EVs. Taken together, this work provides evidence that RWP-1 derived small EVs represent a promising drug delivery tool that can be further investigated in preclinical studies and in clinical trials for the treatment of PDAC.

5. Conclusions

In summary, we have demonstrated that TMZ and EPZ015666 inhibit the growth of RWP-1 cells in vitro by less exposure to the drug when this is loaded in small EVs. Interestingly, we observed that the benefit associated with the use of this natural nanocarrier, depends on the type of the used drug, probably due to the different interactions between the chemical structure of the drug and the extravesicular membrane and this interaction will define its internalization. In this context, our results suggest that TMZ has a better interaction with the lipid bilayer than EPZ015666. Altogether, these results suggest a potential use of RWP-1 derived small EVs as a drug delivery system to obtain the maximum therapeutic effect with minimal toxicity for PDAC patients' treatment.

Funding sources

This study has been funded by Instituto de Salud Carlos III through the project "CP19/00095" (Co-funded by European Social Fund "Investing in your future") and Consellería de Innovación, Universidades, Ciencia y Sociedad Digital from Generalitat Valenciana (CIAICO/2021/135) given to C. d J.R. This study was also funded by Instituto de Salud Carlos III (ISCIII) through the project (PI22/00824) and co-funded by the European Union (FEDER) granted to M.S. and C.d. J.R. FISABIO intramural grants UGP-20–135 also supported this work. S. A.-A. was the recipient of the "Carolina foundation predoctoral fellowship" 2020. R.M. was funded by the Spanish Ministry of Economy and Competitiveness (PID2021–123253OB-C21). E.R.C was financed by the Spanish Ministry of Science, Innovation and Universities PTA2018–015394-I. The FESEM equipment used in this work was funded by the Generalitat Valenciana (Spain) and co-financed with the ERDF funds (OP ERDF of Comunitat Valenciana, Spain) GVA-IDIFEDER_2018/020, "Una forma de hacer Europa". Figures were created in BioRender.com.

CRediT authorship contribution statement

Salomé Araujo-Abad: Conceptualization, Investigation, Methodology, Validation, Formal analysis of data presented in this article, Writing – original draft, Writing – review & editing. **Antonio Manresa-Manresa**: Methodology. **Enrique Rodríguez-Cañas**: Methodology. **María Fuentes- Baile**: Methodology. **Pilar García-Morales**: Writing – review & editing. **Ricardo Mallavia**: Validation, Formal analysis of data presented in this article. **Miguel Saceda**: Writing – review & editing. Camino de Juan Romero: Conceptualization, Funding acquisition, Supervision, Project administration, Validation, Formal analysis of data presented in this article, Writing – original draft, Writing – review & editing. All authors have read and agreed to the published version of the manuscript.

Conflict of Interest Statement

The authors declare that the research was conducted in the absence of any commercial or financial relationships that could be construed as a potential conflict of interest.

Data Availability

Data will be made available on request.

Acknowledgments

The authors thank Ignacio Pachón for assistance with cell culture and Enrique Yuste for the HPLC experiments. We thank Reyes Mateo for sharing reagents. We also thank Maria Irene De La Encarnación Boronat for the English editing of the manuscript.

Appendix A. Supporting information

Supplementary data associated with this article can be found in the online version at doi:10.1016/j.biopha.2023.114657.

References

[1] K.D. Miller, R.L. Siegel, C.C. Lin, A.B. Mariotto, J.L. Kramer, J.H. Rowland, K. D. Stein, R. Alteri, A. Jemal, Cancer treatment and survivorship statistics, 2016, CA Cancer J. Clin. 66 (2016) 271–289, https://doi.org/10.3322/CAAC.21349.
[2] H. Sung, J. Ferlay, R.L. Siegel, M. Laversanne, I. Soerjomataram, A. Jemal, F. Bray, Global cancer statistics 2020: GLOBOCAN estimates of incidence and mortality worldwide for 36 cancers in 185 countries, CA Cancer J. Clin. 71 (2021) 209–249, https://doi.org/10.3322/CAAC.21660.
[3] A. Adamska, A. Domenichini, M. Falasca, Pancreatic ductal adenocarcinoma: current and evolving therapies, Int. J. Mol. Sci. (2017) *18*, https://doi.org/10.3390/IJMS18071338.
[4] J.L. Abbruzzese, Adjuvant therapy for surgically resected pancreatic adenocarcinoma, JAMA 299 (2008) 1066–1067, https://doi.org/10.1001/JAMA.299.9.1066.
[5] C. Fang, K. Wang, Z.R. Stephen, Q. Mu, F.M. Kievit, D.T. Chiu, O.W. Press, M. Zhang, Temozolomide nanoparticles for targeted glioblastoma therapy, ACS Appl. Mater. Interfaces 7 (2015) 6682, https://doi.org/10.1021/AM5092165.
[6] A. Gronchi, A.B. Miah, A.P. Dei Tos, N. Abecassis, J. Bajpai, S. Bauer, R. Biagini, S. Bielack, J.Y. Blay, S. Bolle, et al., Soft tissue and visceral sarcomas: ESMO-EURACAN-GENTURIS clinical practice guidelines for diagnosis, treatment and follow-up, Ann. Oncol. Off. J. Eur. Soc. Med. Oncol. 32 (2021) 1348–1365, https://doi.org/10.1016/J.ANNONC.2021.07.006.
[7] P.G. Casali, S. Bielack, N. Abecassis, H.T. Aro, S. Bauer, R. Biagini, S. Bonvalot, I. Boukovinas, J.V.M.G. Bovee, B. Brennan, et al., Bone sarcomas: ESMO-PaedCan-EURACAN clinical practice guidelines for diagnosis, treatment and follow-up, Ann. Oncol. 29 (2018) iv79–iv95, https://doi.org/10.1093/ANNONC/MDY310.
[8] L.B. Nabors, J. Portnow, M. Ahluwalia, J. Baehring, H. Brem, S. Brem, N. Butowski, J.L. Campian, S.W. Clark, A.J. Fabiano, et al., Central nervous system cancers, version 3.2020, NCCN clinical practice guidelines in oncology, J. Natl. Compr. Canc. Netw. 18 (2020) 1537–1570, https://doi.org/10.6004/JNCCN.2020.0052.
[9] M. von Mehren, J.M. Kane, M.M. Bui, E. Choy, M. Connelly, S. Dry, K.N. Ganjoo, S. George, R.J. Gonzalez, M.J. Heslin, et al., NCCN guidelines insights: soft tissue sarcoma, Version 1.2021, J. Natl. Compr. Cancer Netw. 18 (2020) 1605–1612, https://doi.org/10.6004/JNCCN.2020.0058.
[10] S.M. Swetter, J.A. Thompson, M.R. Albertini, C.A. Barker, J. Baumgartner, G. Boland, B. Chmielowski, D. DiMaio, A. Durham, R.C. Fields, et al., NCCN Guidelines® insights: melanoma: cutaneous, version 2.2021, J. Natl. Compr. Cancer Netw. 19 (2021) 364–376, https://doi.org/10.6004/JNCCN.2021.0018.
[11] M. Pavel, K. Öberg, M. Falconi, E.P. Krenning, A. Sundin, A. Perren, A. Berruti, Gastroenteropancreatic neuroendocrine neoplasms: ESMO clinical practice guidelines for diagnosis, treatment and follow-up, Ann. Oncol. 31 (2020) 844–860, https://doi.org/10.1016/J.ANNONC.2020.03.304.
[12] R. Stupp, M. Brada, M.J. van den Bent, J.C. Tonn, G. Pentheroudakis, High-grade glioma: ESMO clinical practice guidelines for diagnosis, treatment and follow-up, Ann. Oncol. 25 (2014) iii93–iii101, https://doi.org/10.1093/ANNONC/MDU050.
[13] M.J. Moore, R. Feld, D. Hedley, A. Oza, L.L. Siu, A phase II study of temozolomide in advanced untreated pancreatic cancer, Invest. N. Drugs 16 (1998) 77–79, https://doi.org/10.1023/A:1006043332368.
[14] S. Ostermann, C. Csajka, T. Buclin, S. Leyvraz, F. Lejeune, L.A. Decosterd, R. Stupp, Plasma and cerebrospinal fluid population pharmacokinetics of temozolomide in malignant glioma patients, Clin. Cancer Res. 10 (2004) 3728–3736, https://doi.org/10.1158/1078-0432.CCR-03-0807.
[15] S. Sengupta, J. Marrinan, C. Frishman, P. Sampath, Impact of temozolomide on immune response during malignant glioma chemotherapy, Clin. Dev. Immunol. 2012 (2012), 831090, https://doi.org/10.1155/2012/831090.
[16] M.C. Chamberlain, Temozolomide: therapeutic limitations in the treatment of adult high-grade gliomas, Expert Rev. Neurother. 10 (2014) 1537–1544, https://doi.org/10.1586/ERN.10.32.
[17] V.A. Trinh, S.P. Patel, W.-J. Hwu, The safety of temozolomide in the treatment of malignancies, Expert Opin. Drug Saf. 8 (2009) 493–499, https://doi.org/10.1517/14740330902918281.
[18] E. Chan-Penebre, K.G. Kuplast, C.R. Majer, P.A. Boriack-Sjodin, T.J. Wigle, L. D. Johnston, N. Rioux, M.J. Munchhof, L. Jin, S.L. Jacques, et al., A selective

inhibitor of PRMT5 with in vivo and in vitro potency in MCL models, Nat. Chem. Biol. 11 (2015) 432–437, https://doi.org/10.1038/nchembio.1810.
[19] N. Stopa, J.E. Krebs, D. Shechter, The PRMT5 arginine methyltransferase: many roles in development, cancer and beyond, Cell. Mol. life Sci. 72 (2015) 2059, https://doi.org/10.1007/S00018-015-1847-9.
[20] Y. Wang, W. Hu, Y. Yuan, Protein arginine methyltransferase 5 (PRMT5) as an anticancer target and its inhibitor discovery, J. Med. Chem. 61 (2018) 9429–9441, https://doi.org/10.1021/ACS.JMEDCHEM.8B00598/ASSET/IMAGES/LARGE/JM-2018-00598Z_0009.JPEG.
[21] M. Vinet, S. Suresh, V. Maire, C. Monchecourt, F. Némati, L. Lesage, F. Pierre, M. Ye, A. Lescure, A. Brisson, et al., Protein arginine methyltransferase 5: a novel therapeutic target for triple-negative breast cancers, Cancer Med 8 (2019) 2428, https://doi.org/10.1002/CAM4.2114.
[22] A. Singh, C. Fedele, H. Lu, M.T. Nevalainen, J.H. Keen, L.R. Languino, Exosome-mediated transfer of Avβ3 integrin from tumorigenic to nontumorigenic cells promotes a migratory phenotype, Mol. Cancer Res. 14 (2016) 1136–1146, https://doi.org/10.1158/1541-7786.MCR-16-0058.
[23] M. Colombo, G. Raposo, C. Théry, Biogenesis, secretion, and intercellular interactions of exosomes and other extracellular vesicles, Annu. Rev. Cell Dev. Biol. 30 (2014) 255–289, https://doi.org/10.1146/ANNUREV-CELLBIO-101512-122326.
[24] X. Wang, W. Zhong, J. Bu, Y. Li, R. Li, R. Nie, C. Xiao, K. Ma, X. Huang, Y. Li, Exosomal protein CD82 as a diagnostic biomarker for precision medicine for breast cancer, Mol. Carcinog. 58 (2019) 674–685, https://doi.org/10.1002/mc.22960.
[25] S. Araujo-Abad, M. Saceda, C. de Juan Romero, Biomedical application of small extracellular vesicles in cancer treatment, Adv. Drug Deliv. Rev. 182 (2022), 114117, https://doi.org/10.1016/J.ADDR.2022.114117.
[26] L. Qiao, S. Hu, K. Huang, T. Su, Z. Li, A. Vandergriff, J. Cores, P.U. Dinh, T. Allen, D. Shen, et al., Tumor cell-derived exosomes home to their cells of origin and can be used as trojan horses to deliver cancer drugs, Theranostics 10 (2020) 3474–3487, https://doi.org/10.7150/thno.39434.
[27] E.V. Batrakova, M.S. Kim, Using exosomes, naturally-equipped nanocarriers, for drug delivery, J. Control. Release 219 (2015) 396–405, https://doi.org/10.1016/j.jconrel.2015.07.030.
[28] Y. Tian, S. Li, J. Song, T. Ji, M. Zhu, G.J. Anderson, J. Wei, G. Nie, A doxorubicin delivery platform using engineered natural membrane vesicle exosomes for targeted tumor therapy, Biomaterials 35 (2014) 2383–2390, https://doi.org/10.1016/J.BIOMATERIALS.2013.11.083.
[29] L. Nam, C. Coll, L.C.S. Erthal, C. de la Torre, D. Serrano, R. Martínez-Máñez, M. J. Santos-Martínez, E. Ruiz-Hernández, Drug delivery nanosystems for the localized treatment of glioblastoma multiforme, Mater. (Basel) (2018) *11*, https://doi.org/10.3390/MA11050779.
[30] Bazeed, A.Y.; Day, C.M.; Garg, S. Pancreatic Cancer: Challenges and Opportunities in Locoregional Therapies. Cancers 2022, Vol. 14, Page 4257 2022, 14, 4257, doi: 10.3390/CANCERS14174257.
[31] M. Fuentes-Baile, D. Bello-Gil, E. Pérez-Valenciano, J.M. Sanz, P. García-Morales, B. Maestro, M.P. Ventero, C. Alenda, V.M. Barberá, M. Saceda, CLyta-DAAO, free and immobilized in magnetic nanoparticles, induces cell death in human cancer cells, Biomolecules 10 (2020) 222, https://doi.org/10.3390/biom10020222.
[32] M.P. Ventero, M. Fuentes-Baile, C. Quereda, E. Perez-Valeciano, C. Alenda, P. Garcia-Morales, D. Esposito, P. Dorado, V.M. Barbera, M. Saceda, Radiotherapy resistance acquisition in glioblastoma. Role of SOCS1 and SOCS3, PLoS One 14 (2019), e0212581, https://doi.org/10.1371/journal.pone.0212581.
[33] J.L. Neira, S. Araujo-Abad, A. Cámara-Artigas, B. Rizzuti, O. Abian, A.M. Giudici, A. Velazquez-Campoy, C. de Juan Romero, Biochemical and biophysical characterization of PADI4 supports its involvement in cancer, Arch. Biochem. Biophys. 717 (2022), 109125, https://doi.org/10.1016/J.ABB.2022.109125.
[34] D.L. Dexter, G.M. Matook, P.A. Meitner, H.A. Bogaars, G.A. Jolly, M.D. Turner, P. Calabresi, Establishment and characterization of two human pancreatic cancer cell lines tumorigenic in athymic mice, Cancer Res. 42 (1982) 2705–2714.
[35] M. Fuentes-Baile, M.P. Ventero, J.A. Encinar, P. García-Morales, M. Poveda-Deltell, E. Pérez-Valenciano, V.M. Barberá, J. Gallego-Plazas, Á. Rodríguez-Lescure, J. Martín-Nieto, et al., Differential effects of IGF-1R small molecule tyrosine kinase inhibitors BMS-754807 and OSI-906 on human cancer cell lines, Cancers (Basel) 12 (2020) 1–18, https://doi.org/10.3390/cancers12123717.
[36] M. Fuentes-Baile, E. Pérez-Valenciano, P. García-Morales, C. Romero, J. de, D. Bello-Gil, V.M. Barberá, Á. Rodríguez-Lescure, J.M. Sanz, C. Alenda, M. Saceda, Clyta-daao chimeric enzyme bound to magnetic nanoparticles. A new therapeutical approach for cancer patients? Int. J. Mol. Sci. 22 (2021) 1–24, https://doi.org/10.3390/ijms22031477.
[37] M. Fuentes-baile, P. García-morales, E. Pérez-valenciano, M.P. Ventero, J.M. Sanz, C. Romero, J. de, V.M. Barberá, C. Alenda, M. Saceda, Cell death mechanisms induced by CLytA-DAAO chimeric enzyme in human tumor cell lines, Int. J. Mol. Sci. 21 (2020) 1–25, https://doi.org/10.3390/ijms21228522.
[38] Araujo-Abad, S.; Manresa-Manresa, A.; Rodríguez-Cañas, E.; Fuentes-Baile, M.; García-Morales, P.; Mallavia, R.; Saceda, M.; De, C.; Romero, J. Glioblastoma-Derived Small Extracellular Vesicles: Nanoparticles for Glioma Treatment. Int. J. Mol. Sci. 2023, Vol. 24, Page 5910 2023, 24, 5910, doi:10.3390/IJMS24065910.
[39] Y. Zhang, Y. Liu, H. Liu, W.H. Tang, Exosomes: biogenesis, biologic function and clinical potential, Cell Biosci. 9 (2019) 1–18, https://doi.org/10.1186/S13578-019-0282-2.
[40] V. Sokolova, A.K. Ludwig, S. Hornung, O. Rotan, P.A. Horn, M. Epple, B. Giebel, Characterisation of exosomes derived from human cells by nanoparticle tracking analysis and scanning electron microscopy, Colloids Surf. B Biointerfaces 87 (2011) 146–150, https://doi.org/10.1016/J.COLSURFB.2011.05.013.
[41] P. Sarantis, E. Koustas, A. Papadimitropoulou, A.G. Papavassiliou, M. V. Karamouzis, Pancreatic ductal adenocarcinoma: treatment hurdles, tumor microenvironment and immunotherapy, World J. Gastrointest. Oncol. 12 (2020) 173–181, https://doi.org/10.4251/WJGO.V12.I2.173.
[42] D.R. Principe, P.W. Underwood, M. Korc, J.G. Trevino, H.G. Munshi, A. Rana, The current treatment paradigm for pancreatic ductal adenocarcinoma and barriers to therapeutic efficacy, Front. Oncol. 11 (2021) 2773, https://doi.org/10.3389/FONC.2021.688377/BIBTEX.
[43] E.S. Casper, M.R. Green, D.P. Kelsen, R.T. Heelan, T.D. Brown, C.D. Flombaum, B. Trochanowski, P.G. Tarassoff, Phase II trial of gemcitabine (2,2'-difluorodeoxycytidine) in patients with adenocarcinoma of the pancreas, Invest. N. Drugs 12 (1994) 29–34, https://doi.org/10.1007/BF00873232.
[44] J. Carmichael, U. Fink, R.C.G. Russell, M.F. Spittle, A.L. Harris, G. Spiessi, J. Blatter, Phase II study of gemcitabine in patients with advanced pancreatic cancer, Br. J. Cancer 73 (1996) 101–105, https://doi.org/10.1038/BJC.1996.18.
[45] M. Moore, Activity of gemcitabine in patients with advanced pancreatic carcinoma a review BACKGROUND. In early phase I1 trials in advanced pancreatic cancer, Gemcitabine. Cancer 78 (1996) 633–638, https://doi.org/10.1002/(SICI)1097-0142(19960801)78:3<633::AID-CNCR44>3.0.CO;2-X.
[46] J. Robertson, R. Barr, L.N. Shulman, G.B. Forte, N. Magrini, Essential medicines for cancer: WHO recommendations and national priorities, Bull. World Health Organ 94 (2016) 742, https://doi.org/10.2471/BLT.15.163998.
[47] X. Wei, J. Yang, S.J. Adair, H. Ozturk, C. Kuscu, K.Y. Lee, W.J. Kane, P.E. O'Hara, D. Liu, Y.M. Demirlenk, et al., Targeted CRISPR screening identifies PRMT5 as synthetic lethality combinatorial target with gemcitabine in pancreatic cancer cells, Proc. Natl. Acad. Sci. U. S. A. 117 (2020) 28068–28079, https://doi.org/10.1073/PNAS.2009899117/-/DCSUPPLEMENTAL.
[48] C.J. Braun, M. Stanciu, P.L. Boutz, J.C. Patterson, D. Calligaris, F. Higuchi, R. Neupane, S. Fenoglio, D.P. Cahill, H. Wakimoto, et al., Coordinated splicing of regulatory detained introns within oncogenic transcripts creates an exploitable vulnerability in malignant glioma, Cancer Cell 32 (2017) 411–426, https://doi.org/10.1016/J.CCELL.2017.08.018, e11.
[49] X. Liu, J.Z. He, L. Mao, Y. Zhang, W.W. Cui, S. Duan, A. Jiang, Y. Gao, Y. Sang, G. Huang, EPZ015666, a selective protein arginine methyltransferase 5 (PRMT5) inhibitor with an antitumour effect in retinoblastoma, Exp. Eye Res. 202 (2021), 108286, https://doi.org/10.1016/J.EXER.2020.108286.
[50] X.-M. Xi, S.-J. Xia, R. Lu, Drug loading techniques for exosome-based drug delivery systems, Pharmazie 76 (2021) 61–67, https://doi.org/10.1691/ph.2021.0128.
[51] J.Y. Wu, Y.J. Li, X. Hu, Bin, S. Huang, D.X. Xiang, Preservation of small extracellular vesicles for functional analysis and therapeutic applications: a comparative evaluation of storage conditions, Drug Deliv. 28 (2021) 162–170, https://doi.org/10.1080/10717544.2020.1869866/SUPPL_FILE/IDRD_A_1869866_SM9282.DOCX.
[52] R.L. Siegel, K.D. Miller, A. Jemal, Cancer Statistics, 2016, CA Cancer J. Clin. 66 (2016) 7–30, https://doi.org/10.3322/CAAC.21332.
[53] X.Q. Li, J.T. Liu, L.L. Fan, Y. Liu, L. Cheng, F. Wang, H.Q. Yu, J. Gao, W. Wei, H. Wang, et al., Exosomes derived from gefitinib-treated EGFR-mutant lung cancer cells alter cisplatin sensitivity via up-regulating autophagy, Oncotarget 7 (2016) 24585, https://doi.org/10.18632/ONCOTARGET.8358.
[54] Howlader, N.; Noone, A.; Krapcho, M. SEER Cancer Statistics Review (CSR) 1975–2017. National Cancer Institute Available online: https://seer.cancer.gov/archive/csr/1975_2017/ (accessed on 30 September 2022).
[55] National Cancer Institute Surveillance, Epidemiology, and End Results (SEER) Program Available online: https://seer.cancer.gov/statfacts/html/pancreas.html (accessed on 30 September 2022).
[56] T. Conroy, P. Hammel, M. Hebbar, M. Ben Abdelghani, A.C. Wei, J.-L. Raoul, L. Choné, E. Francois, P. Artru, J.J. Biagi, et al., FOLFIRINOX or gemcitabine as adjuvant therapy for pancreatic cancer, N. Engl. J. Med. 379 (2018) 2395–2406, https://doi.org/10.1056/NEJMOA1809775/SUPPL_FILE/NEJMOA1809775_DATA-SHARING.PDF.
[57] J.P. Neoptolemos, D.D. Stocken, H. Friess, C. Bassi, J.A. Dunn, H. Hickey, H. Beger, L. Fernandez-Cruz, C. Dervenis, F. Lacaine, et al., A randomized trial of chemoradiotherapy and chemotherapy after resection of pancreatic cancer, N. Engl. J. Med. 350 (2004) 1200–1210, https://doi.org/10.1056/NEJMOA032295.
[58] A. Laviano, M.M. Meguid, A. Inui, M. Muscaritoli, F. Rossi-Fanelli, Therapy insight: cancer anorexia-cachexia syndrome–when all you can eat is yourself, Nat. Clin. Pract. Oncol. 2 (2005) 158–165, https://doi.org/10.1038/NCPONC0112.
[59] A.J. Grossberg, L.C. Chu, C.R. Deig, E.K. Fishman, W.L. Hwang, A. Maitra, D. L. Marks, A. Mehta, N. Nabavizadeh, D.M. Simeone, et al., Multidisciplinary standards of care and recent progress in pancreatic ductal adenocarcinoma, Ca. Cancer J. Clin. 70 (2020) 375, https://doi.org/10.3322/CAAC.21626.
[60] A. Babic, M.H. Rosenthal, W.R. Bamlet, N. Takahashi, M. Sugimoto, L.V. Danai, V. Morales-Oyarvide, N. Khalaf, R.F. Dunne, L.K. Brais, et al., Post diagnosis loss of skeletal muscle, but not adipose tissue, is associated with shorter survival of patients with advanced pancreatic cancer, Cancer Epidemiol. Biomark. Prev. 28 (2019) 2062, https://doi.org/10.1158/1055-9965.EPI-19-0370.
[61] J.K. Kays, S. Shahda, M. Stanley, T.M. Bell, B.H. O'Neill, M.D. Kohli, M.E. Couch, L. G. Koniaris, T.A. Zimmers, Three cachexia phenotypes and the impact of fat-only loss on survival in FOLFIRINOX therapy for pancreatic cancer, J. Cachex. Sarcopenia Muscle 9 (2018) 673, https://doi.org/10.1002/JCSM.12307.
[62] J. Bachmann, M. Heiligensetzer, H. Krakowski-Roosen, M.W. Büchler, H. Friess, M. E. Martignoni, Cachexia worsens prognosis in patients with resectable pancreatic cancer, J. Gastrointest. Surg. 12 (2008) 1193–1201, https://doi.org/10.1007/S11605-008-0505-Z/TABLES/6.

[63] A. Hendifar, A. Osipov, J. Khanuja, N. Nissen, J. Naziri, W. Yang, Q. Li, R. Tuli, Influence of body mass index and albumin on perioperative morbidity and clinical outcomes in resected pancreatic adenocarcinoma, PLoS One 11 (2016), 152172, https://doi.org/10.1371/JOURNAL.PONE.0152172.

[64] A. Görgens, G. Corso, D.W. Hagey, R. Jawad Wiklander, M.O. Gustafsson, U. Felldin, Y. Lee, R.B. Bostancioglu, H. Sork, X. Liang, et al., Identification of storage conditions stabilizing extracellular vesicles preparations, J. Extracell. Vesicles 11 (2022), e12238, https://doi.org/10.1002/JEV2.12238.

[65] A. Sivanantham, Y. Jin, Impact of storage conditions on EV integrity/surface markers and cargos, Life 12 (2022) 697, https://doi.org/10.3390/LIFE12050697.

[66] Y. Zhang, J. Bi, J. Huang, Y. Tang, S. Du, P. Li, Exosome: a review of its classification, isolation techniques, storage, diagnostic and targeted therapy applications, Int. J. Nanomed. 15 (2020) 6917, https://doi.org/10.2147/IJN.S264498.